Structure-function analysis of Hmo1 unveils an ancestral organization of HMG-Box factors involved in ribosomal DNA transcription from yeast to human

Benjamin Albert[1,2], Christine Colleran[3], Isabelle Léger-Silvestre[1,2], Axel B. Berger[1], Christophe Dez[1,2], Christophe Normand[1,2], Jorge Perez-Fernandez[1,2], Brian McStay[3] and Olivier Gadal[1,2,*]

[1]LBME du CNRS, Université de Toulouse, 118 route de Narbonne, F-31000 Toulouse, France, [2]Laboratoire de Biologie Moléculaire Eucaryote, Université de Toulouse, 118 route de Narbonne, F-31000 Toulouse, France and [3]Centre for Chromosome Biology, School of Natural Sciences, National University of Ireland Galway, University Road, Galway, Ireland

ABSTRACT

Ribosome biogenesis is a major metabolic effort for growing cells. In *Saccharomyces cerevisiae*, Hmo1, an abundant high-mobility group box protein (HMGB) binds to the coding region of the RNA polymerase I transcribed ribosomal RNAs genes and the promoters of ∼70% of ribosomal protein genes. In this study, we have demonstrated the functional conservation of eukaryotic HMGB proteins involved in ribosomal DNA (rDNA) transcription. We have shown that when expressed in budding yeast, human UBF1 and a newly identified Sp-Hmo1 (*Schizosaccharomyces pombe*) localize to the nucleolus and suppress growth defect of the RNA polymerase I mutant *rpa49*-Δ. Owing to the multiple functions of both proteins, Hmo1 and UBF1 are not fully interchangeable. By deletion and domains swapping in Hmo1, we identified essential domains that stimulate rDNA transcription but are not fully required for stimulation of ribosomal protein genes expression. Hmo1 is organized in four functional domains: a dimerization module, a canonical HMGB motif followed by a conserved domain and a C-terminal nucleolar localization signal. We propose that Hmo1 has acquired species-specific functions and shares with UBF1 and Sp-Hmo1 an ancestral function to stimulate rDNA transcription.

INTRODUCTION

Cell growth requires intense protein synthesis activity, making ribosome production the 'house building' function of the cell (1). Transcription by RNA polymerase I (Pol I) of ribosomal RNA (rRNA) genes is thought to be the major rate-limiting step in ribosomes production (2). Although about half of the ribosomal DNA (rDNA) is not transcribed, transcription of the active rRNA genes by Pol I is one to two orders of magnitude greater than the transcription of the rest of the genome. Hmo1 in *Saccharomyces cerevisiae* and UBF in human are highly enriched on actively transcribed rRNA genes (3,4). Furthermore, both have been linked to the regulation of transcription by Pol I (2).

UBF exists as two splice variants, UBF1 and UBF2, each representing ∼50% of UBF in the human cells (5). Both can bind to the rDNA promoter, UBF1 being a more potent activator (6). Numerous functions have been ascribed to UBF1. These include recruitment of the transcription factor SL1 (7), formation of the Pol I preinitation complex (8) and regulation of Pol I's promoter escape during transcription initiation. (9). UBF binding extends from the rDNA promoter region to the entire transcribed region (4,10). Through direct binding to the transcribed region, UBF can also regulate Pol I elongation (11). Tandem arrays of a heterologous high affinity UBF binding site, integrated into human chromosomes, form pseudo-nucleolar organizer regions (NORs) (12). Association of UBF with pseudo-NORs

induces chromatin decondensation and the recruitment of the Pol I machinery (12).

UBF1 contains five high mobility group (HMG) boxes, the first three of which are responsible for binding and loop formation on target DNA (13). It was unlikely that a direct counterpart of UBF is found in yeast. Nevertheless, we previously identified Hmo1, a budding yeast protein bearing one canonical HMG-Box, as a *bona fide* Pol I transcription factor, which has a robust genetic interaction with the specific Pol I subunit Rpa49, the yeast ortholog of the human PAF53 subunit (14,15). Rpa49 has a dual function *in vivo*: it controls the release of the Pol I transcription factor Rrn3 required for initiation of transcription, and it is involved in the elongation of rRNA by Pol I (16–18). In the absence of Rpa49, there is less polymerases on transcribed rDNA genes indicating a defect in initiation (16,19). Deletion of *HMO1* in the *rpa49*Δ strain is lethal, whereas overexpression of Hmo1 suppresses the growth phenotype of *rpa49*Δ (14).

Like UBF, Hmo1 is highly enriched in the nucleolus, bound to the rDNA and implicated in Pol I transcription (14). Unlike UBF, Hmo1 is clearly involved in other processes. Plasmid stability is reduced in *HMO1*-deficient mutants (20). Hmo1 also interacts with TFIID and localizes at Pol II transcription start sites (21). Hmo1 binds ribosomal protein gene (RPG) promoters and regulates their expression (22–24). Furthermore, Hmo1 together with Top2 suppress chromosome fragility during the S phase to preserve genome integrity (25).

In the present study, we directly addressed the functional conservation of these nucleolar high-mobility group box (HMGB) proteins in stimulating Pol I transcription. We show that when expressed in budding yeast, UBF1 and a newly identified Sp-Hmo1 localize to the nucleolus and suppress lethality of the *rpa49*-Δ *hmo1*Δ double mutant. The three proteins Hmo1, Sp-Hmo1 and UBF1 share a similar domains organization. By assessing the ability of truncated or chimeric Hmo1 derivatives to localize to the nucleolus and to restore Hmo1's functions, we have identified a domain in Hmo1, which, when deleted, can uncouple its various functions. Hmo1 is organized into four functional domains; a dimerization module, a canonical HMGB motif followed by a conserved domain and a C-terminal nucleolar targeting signal. If the C-terminal is dispensable for Hmo1 functions, the other motifs are strictly required for Pol I stimulation; importantly, RPG stimulation requires neither the dimerization motif nor the conserved domain.

MATERIALS AND METHODS

Yeast strains, plasmids construction, tetrad analysis and plasmid-shuffling assays

Yeast media and genetic techniques were described previously (26,27). The yeast strains used in this study are listed in Supplementary Table S1, plasmids are listed in Supplementary Table S2 and oligonucleotides are listed in Supplementary Table S3. Yeast strains were constructed by meiotic crossing and transformation with DNA. Complementation was tested using plasmid-shuffling assays. Null alleles of the haploid strains were complemented by the corresponding wild-type (WT) genes borne on *URA3*-containing plasmids. Fluoroorotate (FOA) is toxic for *URA3*+ strains (28). FOA was used to apply a strong positive selection on cells that have lost URA3-containing plasmid bearing WT genes. Ten-fold serial dilutions of each tested strains were spotted on plates with (FOA) or without FOA (−). Growth of strains containing complementing plasmid (without FOA—right panel of each serial dilution) is used as control.

Western blot analyses

Proteins from total cell extracts were separated on 4–20% Tris–glycine polyacrylamide/SDS gels (BioRad) and transferred to hybond-ECL membranes (GE Healthcare). Hmo1 and truncated versions were detected using a polyclonal antibody raised against Hmo1 full-length (kindly provided by Dr Brill) as described in (20) and revealed using Anti-Rabbit IgG horseradish peroxidase (HRP) conjugate (Promega). UBF2, UBF1 and derivatives were detected using 1/3000 dilution of sheep serum raised against UBF1 full-length (12) and revealed using anti-sheep IgG HRP conjugate (abcam). Phosphoglycerate Kinase (PGK) protein level was used as loading control. After detection of the protein of interest, the membrane was washed using antibody striping buffer (GeBA Ltd), incubated with 1/20 000 dilution of mouse PGK antibody (Invitrogen) and revealed using Anti-Mouse IgG HRP conjugate (Promega). All membranes were imaged using LAAS 4000 system (Fujifilm) and processed using MultiGauge V3.0 software.

In vivo labeling, RNA extractions and analysis

Metabolic labeling of pre-rRNAs was performed as previously described (29) with the following modifications. Strains were pre-grown in synthetic glucose containing medium lacking adenine to an optical density at 600 nm of 0.8 at 30°C. One mililiter of cultures were labeled with 50 µCi of [8-^{3}H] adenine (NET06300 PerkinElmer) for 12 min. Cells were collected by centrifugation, and pellets were frozen in liquid nitrogen. RNAs were then extracted as previously described (30) and precipitated with ethanol. For high molecular weight RNAs analysis, 1/5th of the total RNAs were glyoxal denatured and resolved on a 1.2% agarose gel. Low molecular weight RNAs were resolved on 8% polyacrylamide/8.3M urea gels.

Northern blot analysis

RNA extraction and northern hybridization were performed as previously described (30). The oligonucleotides used to detect these RNAs are shown in Supplementary Table S3.

Culture and analysis of human cells

HT1080 were grown in Dulbeco's MEM+GlutaMAX-1 (+4.5 g/l glucose; GIBCO) supplemented with 10% fetal bovine serum (v/v) (BioSera) and 5 U/ml (100 µg/ml) of

penicillin/streptomycin (Sigma). To maintain the 3D-1 cell line (12), the medium was supplemented with 5 µg/ml blasticidinS (Melford). The UBF KD cell line was maintained in medium supplemented with 5 µg/ml blasticidinS and 200 µg/ml Zeocin (Melford). The UBF KD Hmo1 cell line was maintained in medium supplemented with 5 µg/ml blasticidinS, 200 µg/ml Zeocin and 300 µg/ml G418 sulfate (Melford). A full description of the UBF KD cell line can be obtained from B. McStay on request.

Before immuno-fluorescent imaging, cells were grown on Superfrost® Plus microscope slides (Scientific Laboratory Supplies) for at least 24 h. Media was removed, cells were fixed with 4% paraformaldehyde PBS for 10 min at RT, rinsed with PBS and permeabilized with 0.5% saponin and 0.5% Triton X-100 in PBS for 10 min at RT. Antibody incubations were performed for 45–60 min in a humidity chamber at 37°C, followed by washes in PBS. Slides were mounted in Vectashield plus DAPI (Vector Laboratories). Z-stacks of fluorescent images were captured and merged using a Photometric Coolsnap HQ camera and Velocity 5 imaging software (Improvision) with a 63x Plan Apochromat Zeiss objective mounted on a Zeiss Axioplan2 imaging microscope.

Electron microscopy

For morphological analysis of nucleoli, yeast were cryofixed by high-pressure freezing (EMPACT, Leica) and cryosubstituted with OsO_4 0.02%, Uranyl Acetate 0.1%, glutaraldehyde 1% in acetone, for 72 h. Cells are then embedded in a Lowicryl resin (HM-20) polymerised at −50°C. Sections of 100 nm were analysed with a Jeol 1200X electron microscope. Manual segmentation of nucleus, nucleolus and dense fibrillar component and measurement of their size were performed using ImageJ on 20 nuclei for each background (http://rsb.info.nih.gov/ij/).

Immunofluorescence

Immunofluorescence was performed according to (31). *Schizosaccharomyces pombe* cells were then incubated at room temperature with a polyclonal primary antibody (67 724) against Gar2 at ¼ dilution in buffer B (31) for 2 h followed by 1 h of incubation with a primary monoclonal antibody anti-HA. Fluorescent detection was achieved with an incubation of both the secondary antibodies, Alexa Fluor 594-conjugated goat anti-rabbit IgG and the Alexa Fluor® 488 goat anti-mouse. For Hmo1 detection, *S. cerevisiae* cells were incubated overnight at 4°C with rabbit antiserum against Hmo1 at 1/300 dilution (20). Fluorescence detection was performed using Texas Red conjugated goat anti-rabbit IgG (Santa Cruz biotechnology Inc.).

Fluorescence microscopy and image analysis

Wide-field fluorescent images were captured with an Olympus IX-81 microscope equipped with Polychrome V monochromator, Coolsnap HQ camera (Rooper) controlled with Metamorph acquisition software V6 (Universal Imaging). Confocal Microscopy was performed with an Andor Revolution Nipkow-disk confocal system installed on an Olympus IX-81, featuring a CSU22 confocal spinning disk unit (Yokogawa) and an EMCCD camera (DU 888, Andor). Pixel size was 65 nm. For 3D analysis, Z-stacks of 41 images with a 250 nm Z-step were used. Exposure time was 200 ms. Confocal images were processed and analyzed with a Matlab script nucloc, available at http://www.nucloc.org/ (MathWorks) (32).

Chromatin immunoprecipitation

Exponentially growing cells were treated with formaldehyde 1% final concentration during 15 min. Cells were lysed using glass beads in Precellys24 (Precellys). To keep rDNA in the soluble fraction, samples were rotated for 5 min at low speed (1000g at 4°C) (33). Antibodies used were anti-HA (12CA5; Babco.) Immunoprecipitated DNA was quantified by PCR monitored in real time. Each immunoprecipitation sample is normalized to an input sample to control for experimental variations.

RESULTS

UBF1 is nucleolar when expressed in yeast

To determine whether Hmo1 and human UBF have conserved functions *in vivo*, we individually expressed UBF isoforms, UBF1 and UBF2, in a WT yeast strain. In *S. cerevisiae*, YFP tagged UBF1 and UBF2 were localized predominantly in a crescent shaped structure flanking the nuclear envelope and occupying about one-third of the nuclear volume, reminiscent of the yeast nucleolar structure (Figure 1A and B). Co-expression of YFP-UBF1 with fluorescently tagged Hmo1 and Nop1 (the yeast paralog of human fibrillarin) confirmed its nucleolar targeting. (Figure 1B, upper panel) (14). Surprisingly, in contrast to a WT strain, on expression of YFP-UBF1, Hmo1-CFP and mRFP-Nop1 appeared to be fully co-localized *in vivo* (14). Moreover, the nucleolar region appeared larger (Figure 1B, lower panel; YFP-UBF2, not shown). This effect is reversed when YFP-UBF1 expressing construct is omitted (data not shown), indicating that the presence of YFP-UBF1 is solely responsible of the modified nucleolar morphology.

To relate nucleolar enlargement to function, we investigated nucleolar size in WT cells overexpressing Hmo1, UBF1 or UBF2. Nuclear and nucleolar volumes were measured using signals for the nuclear pore protein GFP-Nup49 and the nucleolar mRFP-Nop1, respectively (32). Visual inspection of nucleolar morphology suggests that UBF2, like UBF1, but not Hmo1 overexpression, results in enlarged nucleolus (Figure 1C). When measuring nuclear to nucleolar volumes ratio in a large number of cells, we could confirm a significant increase of nucleolar volume in both UBF1 and UBF2 expressing strains and a reduced nucleolar volume on Hmo1 overexpression (see 'Materials and Methods' section; Figure 1D). Nucleolar expansion caused by UBF1 expression appears to be largely a consequence of dense fibrillar component enlargement as estimated by electron microscopy (see Supplementary Figure S1).

In conclusion, the nucleolar localization of UBF1 and UBF2 suggests that they could have a function in the yeast
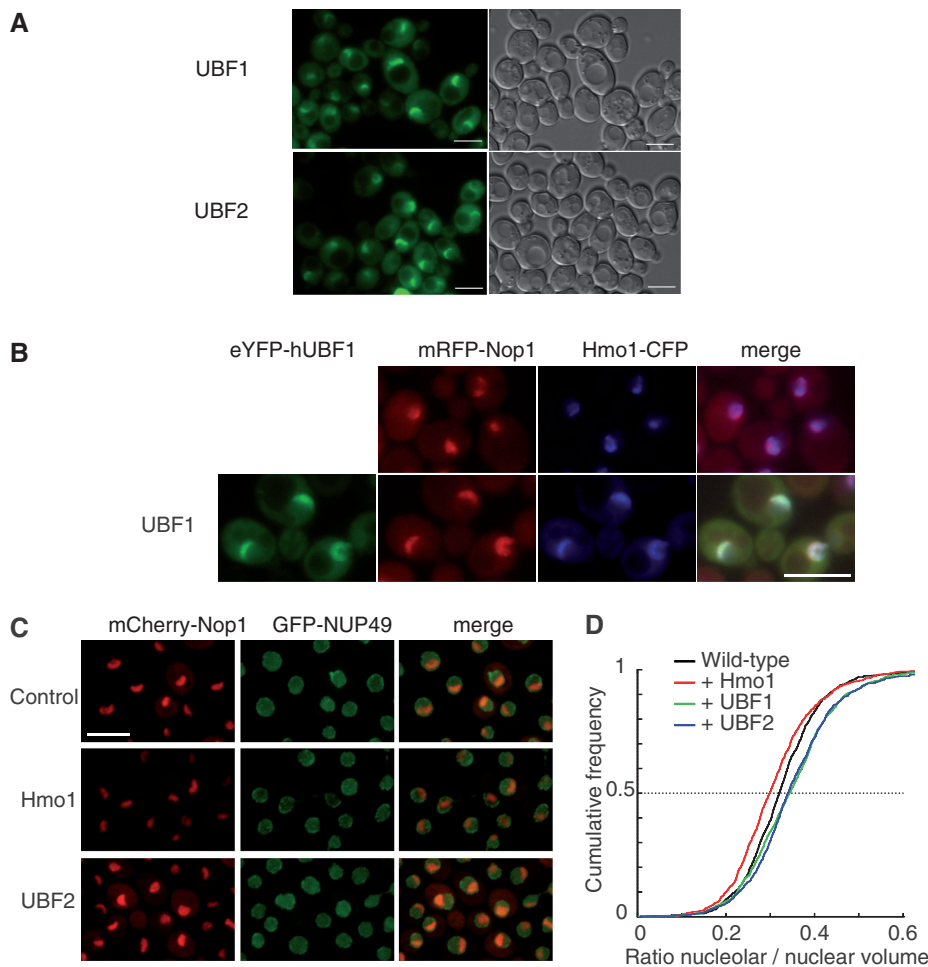
Figure 1. When expressed in *S. cerevisae*, UBF1 and UBF2 are nucleolar and increase nucleolar volume. (**A**) UBF1 and UBF2 fused to YFP and produced in yeast concentrate in a nuclear crescent shape structure. (**B**) The construct encoding the YFP-UBF1 fusion protein (green) was used to transform a strain producing a Hmo1-CFP fusion protein (blue) and an mRFP-Nop1 fusion protein (red), which define different subdomains of the nucleolus. UBF1, Hmo1 and Nop1 fully co-localize. (**C**) A strain producing mRFP-Nop1 fusion protein (red) and GFP-Nup49, which reveals the nucleolus and nuclear, respectively, periphery was transformed with empty plasmid (Control), a plasmid over-expressing Hmo1 or UBF1 (not shown) or UBF2. (**D**) Nuclear and nucleolar volumes were imaged by confocal microscopy and quantified using automated detection software (32). Cumulative frequency plots of the nucleolar to nuclear volumes ratio show a decrease on Hmo1 overexpression [Two-sample Kolmogorov–Smirnov test (KS), $P = 2.7\mathrm{e}^{-06}$] and a significant increase on UBF1 (KS test, $P = 1.6\mathrm{e}^{-08}$) or UBF2 (KS test, $P = 4.3\mathrm{e}^{-07}$) expression relative to control. Scale bar is 5 μm.

nucleolus. However, in contrast to Hmo1 overexpression, expression of UBF1 and UBF2 led to nucleolar enlargement, which can be an indirect consequence of heterologous expression of human proteins.

UBF1 functionally substitutes for Hmo1 in rDNA but not in RPGs transcription

UBF1, but not UBF2, can stimulate rDNA transcription in mammalian cells and *in vitro* (34,35). We tested if human UBF1 and UBF2 are toxic in WT budding yeast and if UBF1 or UBF2 can substitute for Hmo1. We expressed untagged human UBF1 or UBF2 in WT yeasts and in an *hmo1Δ* mutant background (Figure 2A). Despite the apparent nucleolar enlargement on UBF expression in WT cells, no growth defect is observed on UBF1 or UBF2 expression (Figure 2B, left panel). No significant rescue of the growth defect of *hmo1Δ* could be detected,

showing that neither UBF1 nor UBF2 can fully substitute for Hmo1 *in vivo* (Figure 2B, middle panel). We next tested whether UBF could substitute for one of the functions of Hmo1. Functions of Hmo1 can be uncoupled by genetic means, using three different double mutant backgrounds: *hmo1Δ-rpa34Δ*, *hmo1Δ-rpa49Δ*, *hmo1Δ-rps23bΔ*. Rpa34 is a fully dispensable subunit of Pol I, ortholog to human PAF49/CAST subunit (36,37). The double mutant *hmo1Δ-rpa34Δ* has a synthetic slow growth phenotype, exacerbating the Pol I defect of *hmo1Δ* single mutant (24). We expressed UBF1 or UBF2 in *hmo1Δ-rpa34Δ* double mutant. In this mutant background, UBF1, but not UBF2 could alleviate the growth defect of the double mutant (Figure 2B, right panel). To confirm that UBF1 actually stimulates yeast Pol I activity, we expressed UBF1 in an *hmo1Δ rpa49Δ* double mutant. Viability in the *hmo1Δ rpa49Δ* double mutant is maintained by a plasmid bearing *RPA49*, which can be counter selected
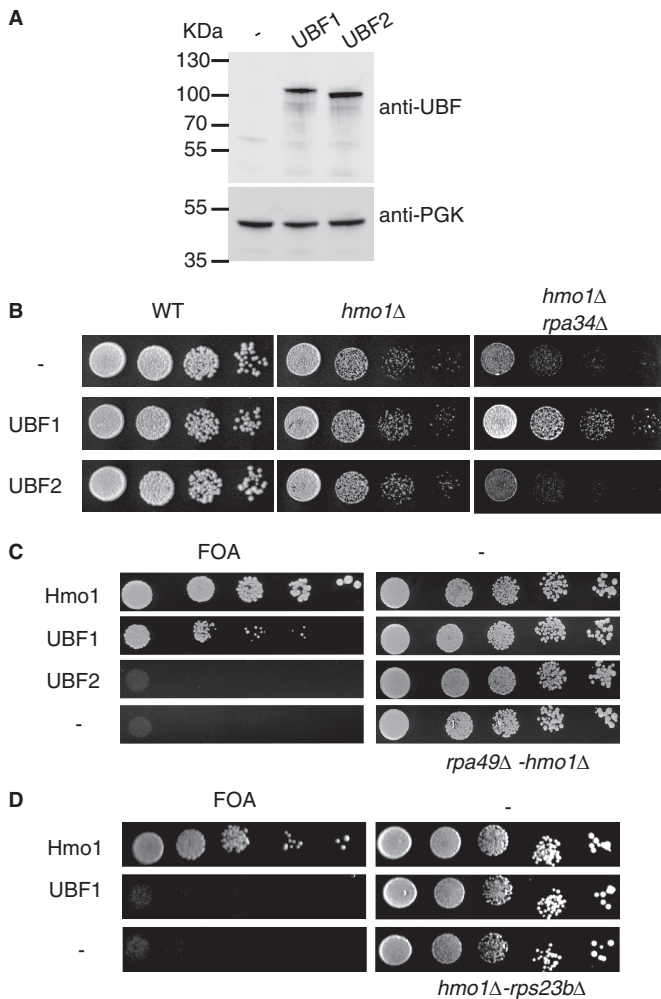
A

B

C

D

Figure 2. UBF1 can stimulate growth of the *rpa49Δ-hmo1Δ* mutant. (**A**) UBF1 and UBF2 are expressed at similar level in budding yeast as estimated by western blot. Total proteins were extracted from WT strain bearing an empty plasmid (−), expressing UBF1 or UBF2. PGK1 was used as loading control. (**B**) UBF1, but not UBF2, partially complements the growth defect of *rpa34Δ-hmo1Δ* strain. WT, *hmo1Δ* and *hmo1Δ-rpa34Δ* double mutant expressing UBF1 or UBF2 were spotted on minimum media, and growth was scored after 3 days at 25°C. (**C**) UBF1 complements the essential functions of Hmo1 in *rpa49Δ-hmo1Δ*. Ten-fold serial dilutions of the double *rpa49-hmo1* deleted strain expressing Hmo1, UBF1, UBF2 or bearing an empty vector (−) were spotted on plates containing 5-FOA to test for complementation (see 'Materials and Methods' section). (**D**) Double *hmo1Δ-rps23bΔ* deleted strain expressing Hmo1, UBF1 or an empty vector (−) were spotted on plates containing 5-FOA to test for complementation. Plates without FOA (−) were used as controls to confirm that similar numbers of cells were spotted.

on FOA containing medium (see 'Materials and Methods' section). Importantly, lethality of *hmo1-Δ rpa49-Δ* double mutant is circumvented when 35S pre-rRNA is produced by RNA polymerase II, showing that lethality in this double mutant is due to defective Pol I transcription (14). Our results show that UBF1 but not UBF2 expression restored growth of the *hmo1Δ rpa49Δ* double mutant (Figure 2C).

Hmo1 is bound to 70% of RPG promoters, but a *hmo1* deleted mutant has only mild effect on most RPG

expression (22–24). On a few RPGs, Hmo1 deletion has a marked effect on the expression of one of the two copies (e.g. *RPS16A* or *RPS23A*). Therefore, *hmo1* deletion becomes lethal when combined with deletion of the other copy of the genes (e.g. *RPS16B* or *RPS23B*). Using such a double mutant (*hmo1Δ-rps23bΔ*), we could show that UBF1 expression could not rescue RPG stimulation in absence of Hmo1 (Figure 2D).

UBF1 and Hmo1 both stimulate rDNA transcription in budding yeast

In mammals, UBF1 stimulates both initiation and elongation step of the Pol I transcription cycle (38). In yeast, deletion of Rpa49 is associated with defects in Pol I initiation and elongation (16–18). Overexpression of Hmo1 in *rpa49-Δ* single mutant increases growth rate and stimulates rRNA synthesis (14). Similarly, UBF1 expression could stimulate growth in *rpa49Δ* strain, even in the presence of endogenous Hmo1 (Figure 3A).

To relate the growth stimulation upon UBF1 expression with rRNA synthesis, we performed metabolic labeling of newly synthesized RNA (Figure 3B). To discriminate between preferential stimulation of initiation or of elongation, we performed Pol I's chromatin immunoprecipitation (ChIP) (Figure 3C). We achieved both experiments in the *rpa49Δ* mutant containing only 25 rDNA genes, all active in transcription, allowing an easier interpretation of our observations (16,39). We checked that in such a background, both overexpression of Hmo1 and heterologous expression of UBF1 could also suppress *rpa49Δ* growth defect (data not shown). In our metabolic labeling of RNA, 5S rRNA and tRNA both transcribed by RNA polymerase III, were used as labeling controls (Figure 3B). Our results show that rRNA production is drastically reduced in *rpa49Δ* mutant compared with WT and partially restored on UBF1 expression. Therefore, just like Hmo1 overexpression (14), UBF1 expression in budding yeast stimulates rRNA production in *rpa49Δ* mutant (Figure 3B).

The results of ChIP experiments showed that compared with WT, *rpa49* deletion reduced Pol I occupancy by ∼3-fold (18) (Figure 3C). Pol I global loading rate and 5′ relative to 3′ Pol I density over rDNA genes should be differentially affected depending on whether initiation or elongation is restored when expressing Hmo1 or UBF1 in an *rpa49Δ* mutant (11,40). Overexpression of Hmo1 and UBF1 in *rpa49Δ* background did not change significantly Pol I loading rate per active gene or the 5′ to 3′ Pol I loading ratio (Figure 3C). These results suggest that Hmo1 or UBF1 are probably able to alleviate the *rpa49Δ* defect in rRNA synthesis without preferential stimulation of initiation relative to elongation.

N-terminal part of UBF1 is sufficient to stimulate rDNA transcription in budding yeast

UBF1 is a much larger protein than Hmo1 and has a well-established domain structure that includes: an N-terminal dimerization domain (UBF-D), five conserved HMG boxes (with the first being the most canonical) followed by a negatively charged C-terminal motif (41) (Figure 4A).
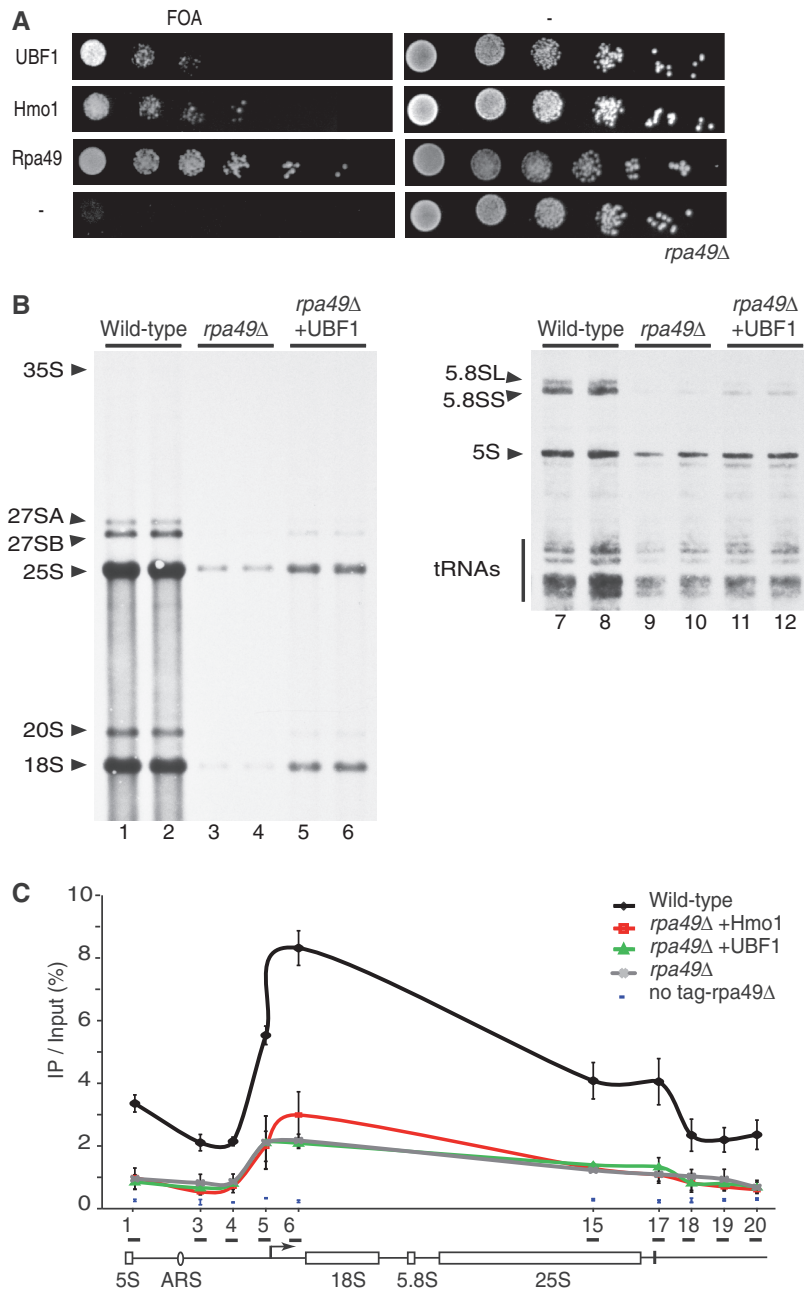
Figure 3. UBF1 and Hmo1 stimulate rDNA transcription in budding yeast. (**A**) Ten-fold serial dilutions of the *rpa49* deleted strain expressing Hmo1, UBF1, *RPA49* or an empty vector (−) were spotted on plates containing 5-FOA and incubated at 25°C for 5 days to test for complementation of *rpa49Δ* growth defect. (**B**) *In vivo* labeling of newly synthesized RNAs. Two different clones of WT (lanes 1–2 and 7–8), *rpa49Δ* (lanes 3–4 and 9–10) and *rpa49Δ* strains expressing UBF1 (lanes 5–6 and 11–12) were grown to an OD600 of 0.8. Cells were then pulse-labeled with [$^{8-3}$H] adenine for 12 min. Samples were collected and total RNAs were extracted, separated by gel electrophoresis. High molecular weight RNAs were resolved on an agarose gel (left panel, lanes 1–6), low molecular weight RNAs were resolved on a polyacrylamide gel (right panel, lanes 7–12). (**C**) Effect of Hmo1 and UBF1 overexpression on rDNA occupancy by Pol I. ChIP assays were performed on a strain with 25 rDNA copies expressing a HA-tagged version of the largest subunit of Pol I, Rpa190 and deleted for *RPA49* (*rpa49Δ*, gray line). This strain is transformed with the appropriate plasmids allowing expression of Rpa49 (complemented WT, black line), overexpression of Hmo1 (*rpa49Δ*+Hmo1; red line) or overexpression of UBF1 (*rpa49Δ*+UBF1; green line). Pol I was pull-down by anti-HA antibodies. ChIP from untagged strains is used as background binding (no tag). DNA occupancy was defined by the ratio between the immunoprecipitation (IP) and the input signals. The bottom diagram shows the positions of the primers used for qPCR amplification on rDNA. The arrow denotes the start site and transcription orientation of the 35S rRNA gene.

Importantly, the C-terminal domain of UBF is thought to be required for stimulation of initiation via an interaction with the human initiation factor SL1 (42). We therefore sought to identify the minimum domains within UBF1 required for nucleolar localization and Pol I stimulation in yeast. Interestingly, UBF1 and UBF2 are both nucleolar. However, only UBF1 was able to substitute Hmo1's function in Pol I mutant. UBF2 is a shorter spliced variant

of UBF1, in which the functional HMG Box2 is missing (5). The N-terminal dimerization module and the two first HMG boxes of UBF1 are sufficient for binding and bending the rDNA (13,42). We hypothesized that N-terminal part of UBF1 (UBF-Box1-2) could be sufficient in yeast to substitute Hmo1 function in Pol I transcription. To test this hypothesis, we expressed truncated forms of UBF1: UBF-Box1 and UBF-Box1-2 in a *S. cerevisiae* WT strain expressing CFP-Nup49 to delineate the nuclear envelope and mCherry-Nop1 to label the nucleolus (Figure 4B). Both proteins localized in the yeast nucleolus (Figure 4B). To test the ability to stimulate Pol I activity, we expressed both untagged UBF-Box1 and UBF-Box1-2 in the *hmo1Δ rpa49Δ* background (Supplementary Figure S2A). Only UBF-Box1-2 rescued growth albeit not as efficiently as UBF1 full length (Figure 4C). Therefore, N-terminal region of UBF1 (including the functional Box 2 absent in UBF2) is sufficient to stimulate Pol I activity in absence of Hmo1 in rpa49 null mutant.
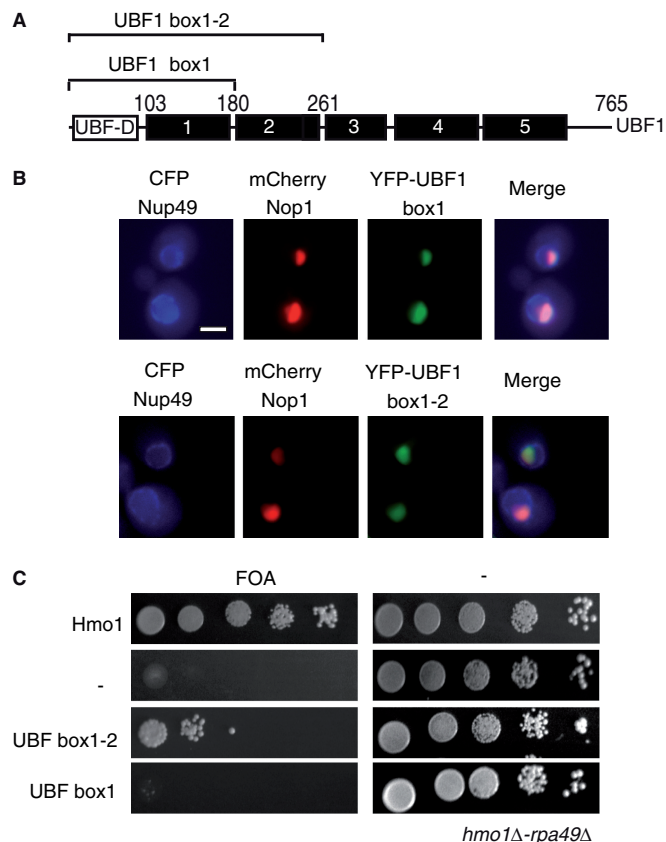

Figure 4. UBF1 N-terminal domain is sufficient to rescue viability of *rpa49Δ-hmo1Δ* strain. (**A**) Schematic representation of UBF1. UBF1 depicted as an N-terminal dimerization domain (UBF-D) and five HMG Boxes (1–5). Truncated UBF1 constructions, Box1 and Box1-2, are shown by square brackets. (**B**) YFP-truncated proteins were co-expressed with CFP-Nup49 and mRFP-Nop1 fusion proteins that, respectively, delineate the nuclear periphery (blue) and the nucleolus (red). Truncated UBF1 constructions Box1 and Box1-2 localized in the yeast nucleolus. (**C**) UBF1-Box1-2 is sufficient to stimulate Pol I. Ten-fold serial dilutions of the *rpa49Δ-hmo1Δ* strain expressing the UBF1 truncation Box1, Box1-2, or Hmo1 or an empty vector (−) were spotted onto plates containing 5-FOA to test for complementation (see 'Materials and Methods' section).

A nucleolar HMGB protein stimulates Pol I transcription in *S. pombe*

In budding yeast and human, Pol I activity requires an HMGB factor. To test for the existence of an ancestral HMGB factor stimulating Pol I activity in all eukaryotes, we next tried to identify by sequence similarity a putative counterpart in a distantly related eukaryote, *S. pombe*. Owing to an overall low sequences similarity between Hmo1 and UBF1, the conserved region (CR) between Hmo1 and UBF1 is limited to a consensus HMGB motif followed by 40 amino acids (Figure 5A). In the *S. pombe* proteome, we tested four HMGB proteins, each containing HMGB motifs (Figure 5B). We produced each of those four HMGB proteins fused to YFP in a WT *S. cerevisiae* strain expressing CFP-Nup49 and mCherry-Nop1:only Spbc28F2.11 accumulated in the nucleolus (Figure 5C). We next produced the four untagged proteins in the *S. cerevisiae hmo1Δ rpa49Δ* double mutant (Figure 5D): Spbc28F2.11 restored growth of the double mutant in contrast to the other HMGB proteins. Moreover, like UBF1, Spbc28f2.11 cannot substitute for Hmo1 in *hmo1Δ rps23bΔ* double mutant (Figure 5E). This heterospecific complementation assay suggests that Spbc28f2.11, hereafter called Sp-Hmo1, could act as a Pol I transcription factor.

We then tested whether Sp-Hmo1 is nucleolar and does influence Pol I activity in *S. pombe*. HA-tagged Sp-Hmo1 was detected by immunofluorescence in WT *S. pombe*; the fluorescent signal was concentrated in the nucleolus as indicated by co-localization with Gar2 an abundant nucleolar protein (Figure 6A). Next, we generated a Sp-Hmo1 gene deletion in *S. pombe*. In *S. cerevisiae*, Hmo1 is required for growth at 25°C and a hmo1Δ mutant strain accumulates unprocessed 35S rRNA, suggesting a direct or indirect rRNA processing defect (23). In contrast to *HMO1* deletion in *S. cerevisiae*, deletion of *Sp-HMO1* in *S. pombe* did not affect growth (data not shown). We analyzed the effect of Sp-HMO1 deletion on ribosome biogenesis by northern blot analysis to assess the steady-state content of rRNA precursors. The deletion resulted in a mild depletion of the two earliest precursors, 35S and 32S rRNA, but little or no effect on the accumulation of other downstream precursors (27SA, 27SB$_L$ 27B$_S$ and 20S rRNA) when compared with WT cells (Figure 6B). Therefore, deletion of *Sp-HMO1* impacts accumulation of early rRNA precursors.

In *S. cerevisiae*, stimulation of rRNA production by Hmo1 was uncovered in one Pol I mutant: in the absence of specific Pol I subunit Rpa49, Hmo1 becomes essential and its overexpression suppresses the *rpa49Δ* growth defect at 25°C (14). We tested whether this genetic link is conserved in *S. pombe*. The *S. pombe* ortholog of the budding yeast Rpa49 is Rpa51, hereafter termed Sp-Rpa49 (43). We crossed the *S. pombe* haploid single mutants *Sp-hmo1Δ* and *Sp-rpa49Δ* and tried to isolate double-deletion mutants after meiosis. None of the 64 offsprings were double mutants, suggesting that *Sp-HMO1* and *Sp-RPA49* deletions are synthetically lethal in *S. pombe* (Figure 6C). *Sp-RPA49* deletion strain was unable to grow at 25°C and overexpression of
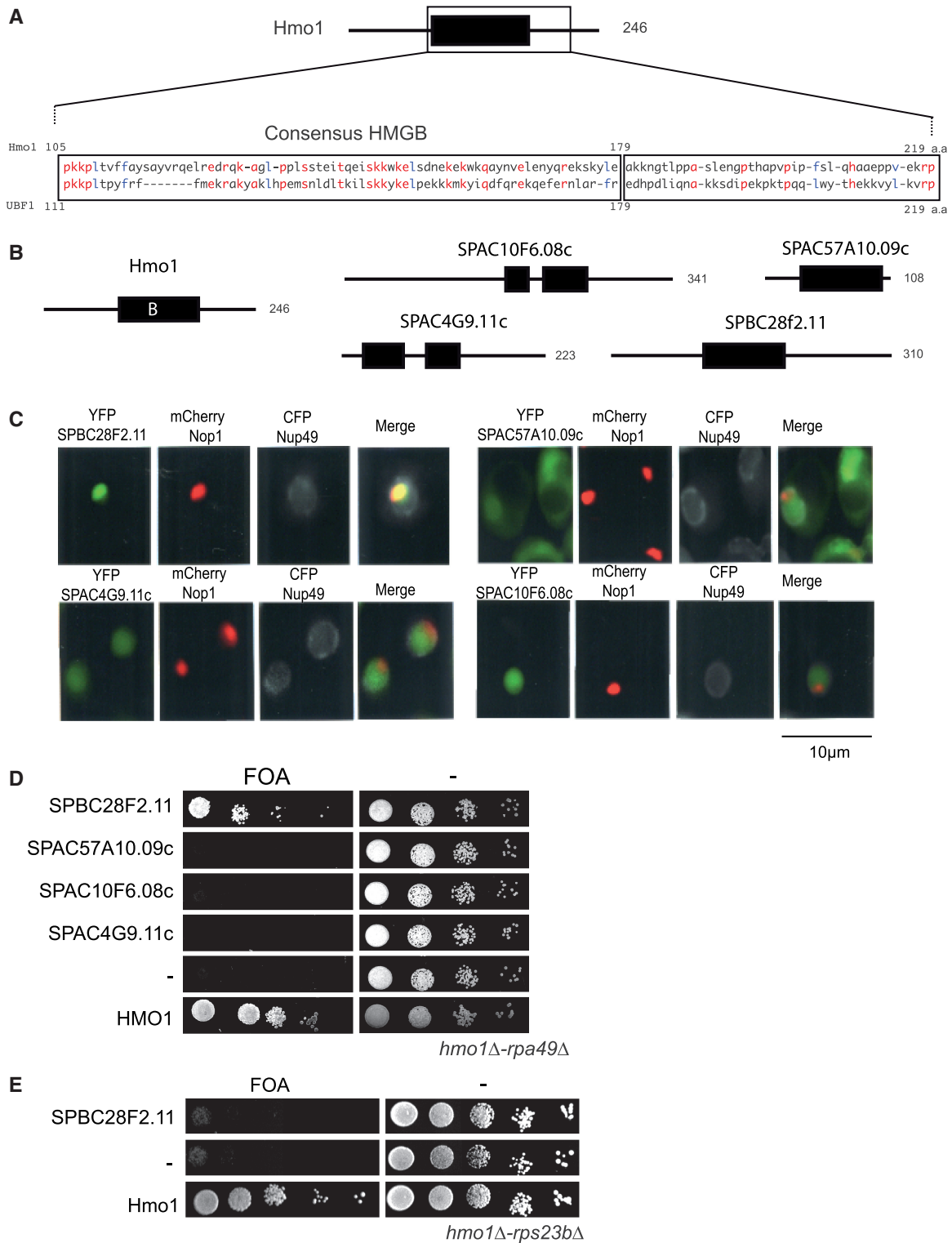
Figure 5. Identification of a Hmo1 counterpart in *S. pombe*. (**A**) Schematic representation of Hmo1. The position of the consensus HMGB region B (black rectangle) is shown in the schematic representation of Hmo1 and the amino-acid compositions of UBF1 and Hmo1 are presented in the close-up view. Residues that are identical are written in red and conserved hydrophobic residues are written in blue. (**B**) Localization of the HMGB of Hmo1 (black rectangle) and in four *S. pombe*'s proteins (Spbc28f2.11, Spac10f6.08c, Spac4g9.11c, Spac57a10.09c). Number of amino acids of each protein is indicated. (**C**) Spbc28f2.11 localizes to the nucleolus when expressed in budding yeast. The four HMGB proteins from *S. pombe* were co-expressed in *S. cerevisiae* as YFP fusion proteins (green) with CFP-Nup49 (gray) and mRFP-Nop1 (red) fusion proteins to visualize the nuclear periphery and the nucleolus, respectively (**D**) Spbc28f2.11 can substitute for the essential function of Hmo1 in a *rpa49Δ-hmo1Δ* background. Ten-fold serial dilutions of cultures of the *rpa49Δ-hmo1Δ* mutant expressing Hmo1, one HMGB from *S. pombe* or an empty vector (−) were spotted on plates containing 5-FOA to test for complementation. (**E**) Spbc28f2.11 cannot substitute for the essential function of Hmo1 in a *hmo1Δ-rps23bΔ* background. Ten-fold serial dilution of cultures of the *rps23bΔ-hmo1Δ* mutant expressing Hmo1, Spbc28f2.11 or an empty vector (−) were spotted on plates containing 5-FOA to test for complementation.
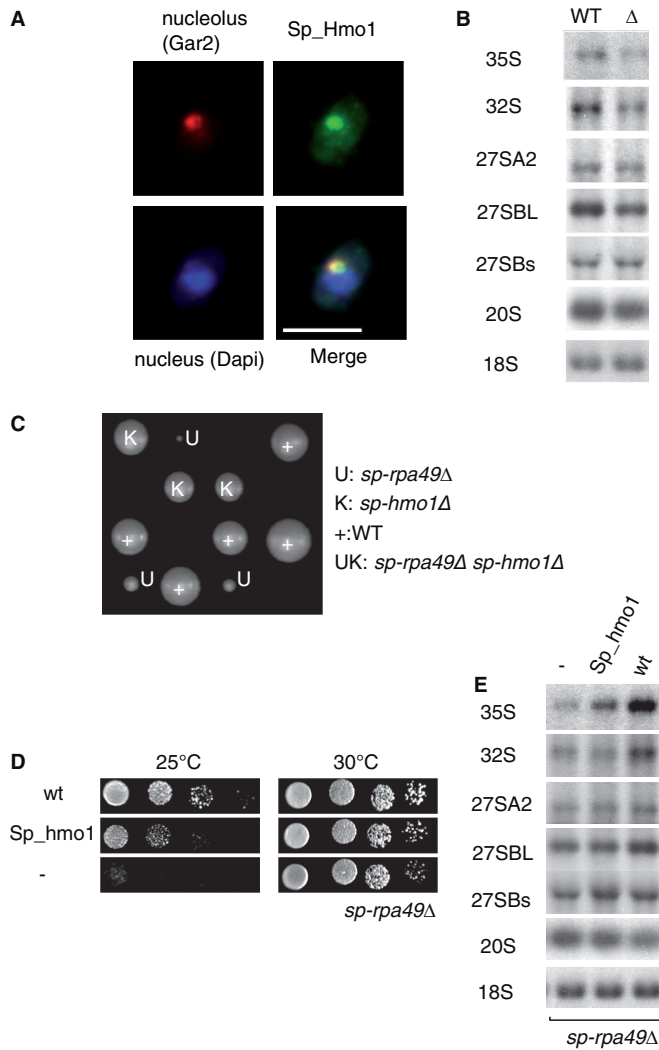
Figure 6. Characterization of the Hmo1 counterpart in *S. pombe*. (**A**) Localization of Sp-Hmo1 in *S. pombe*. Sp-Hmo1 was produced as a C-terminal HA-tagged protein in *S. pombe* and detected by immunofluorescence (green). The nucleolus was revealed by immunodetection of the Gar2 protein (red) and DAPI labeled the nucleus (blue). Scale bar 5 μm (**B**) Sp-Hmo1 is required for 35S pre-rRNA accumulation. Total RNA was extracted from a WT strain and Sp-*hmo1*Δ (Δ) mutant cells and analyzed by northern blotting. Hybridizations revealed the precursors indicated on the left of each panel. (**C**) The *Sp-hmo1*Δ-*Sp-rpa49*Δ double mutant is not viable. After mating of haploid *Sp-hmo1*Δ and *Sp-rpa49*Δ strains and meiosis, growth of segregants bearing *Sp-hmo1*Δ (K) and *Sp-rpa49*Δ (U) was followed by tetrad analysis. WT and single mutants *Sp-hmo1*Δ and *Sp-Rpa49*Δ were selected with KAN (K) and URA3 (U); their frequencies are close to those expected, but no double mutant was isolated. (**D**) Overexpression of Sp-Hmo1 suppresses the growth defect of *Sp-rpa49*Δ at 25°C. The *Sp-rpa49*Δ mutant transformed with empty vector (−), Sp-RPA49 complementing the deletion (WT) or Sp-HMO1 driven from a strong promoter were grown for 4 days at 25°C or 30°C. (**E**) Accumulation of rRNA precursors was restored in the *Sp-rpa49*Δ mutant by overexpression of Sp-Hmo1. Total RNA was extracted and analyzed by northern blotting. Hybridizations revealed the precursors indicated on the left of each panel.

Sp-Hmo1 from the strong *NMT1* promoter effectively suppressed this growth defect (Figure 6D). We used northern blotting to analyze the steady-state content of rRNA precursors in *S. pombe* WT and *Sp-rpa49*Δ to confirm that Sp-Hmo1 suppression results in a modification of rRNA production. Accumulation of the unprocessed Pol I transcript 35S rRNA is strongly impaired in *Sp-rpa49*Δ compared with WT. The 35S accumulation is partially recovered on Sp-Hmo1 overexpression with no observable effect on other downstream precursors. Thus, growth-phenotype suppression of the *Sp-rpa49*Δ by Sp-Hmo1 overexpression correlates with recovery of WT accumulation level of the pol I primary transcript (35S rRNA) (Figure 6E).

We conclude that Sp-Hmo1, although fully dispensable for growth, can stimulate Pol I activity and our genetic analysis suggests that it is a functional equivalent of Hmo1 for rDNA transcription in *S. pombe*.

Consequences of Hmo1 expression in human cells

We have shown that UBF1 expression in yeast can partially substitute for Hmo1. To study the functional conservation of Hmo1 and UBF1 in more detail, we introduced a Hmo1 expression plasmid into the human cell line HT1080. We observed that Hmo1 co-localized with UBF in nucleoli with a low nucleoplasmic signal (Figure 7A). Like UBF, Hmo1 was concentrated on NORs on metaphase chromosomes (Figure 7A) (44). As rDNA transcription is reduced or even stopped during mitosis of mammalian cells, this observation supports the observation that, like UBF, Hmo1 associates with ribosomal gene chromatin even in the absence of Pol I transcription (44,45). We next produced Hmo1 in a cell line (3D-1) bearing a pseudo-NOR (12). Pseudo-NORs detected by immunofluorescence appear as novel sub-nuclear bodies, distinct from nucleoli. They sequester a significant fraction of many components of the Pol I transcription machinery, including UBF. Pseudo NORs lack Pol I promoter sequences and are therefore transcriptionally silent and do not recruit RNA-binding factors such as nucleolin or fibrillarin. When produced in small amounts in 3D-1 cells, Hmo1 was sequestered by pseudo-NORs (Figure 7A), providing further evidence that Hmo1 can be recruited directly to ribosomal genes chromatin in human cells.

UBF is essential for cell growth and proliferation, as shown by shRNA-mediated depletion (Figure 7B and C). A growth arrest phenotype is observed on activation of a tetracycline inducible shRNA targeting both UBF1 and UBF2 in the human cell line HT1080. By introduction of a tetracycline-inducible Hmo1 expression vector, we could simultaneously abolish UBF production and induce Hmo1 production (Figure 7B). In this system, we could test whether Hmo1 can replace UBF1 function in human cells. UBF has multiple roles in the Pol I transcription cycle, including at the initiation step of rDNA transcription and during elongation (9,11). In this work, we have shown that the common function between Hmo1 and UBF1 does not preferentially stimulate initiation rather than elongation (Figure 3), and we have proposed that N-terminal part of UBF1 could be equivalent to Hmo1 (Figure 4). In our system of complementation, Hmo1 did not overcome the growth arrest associated with UBF depletion (Figure 7C). This result shows that UBF fulfills
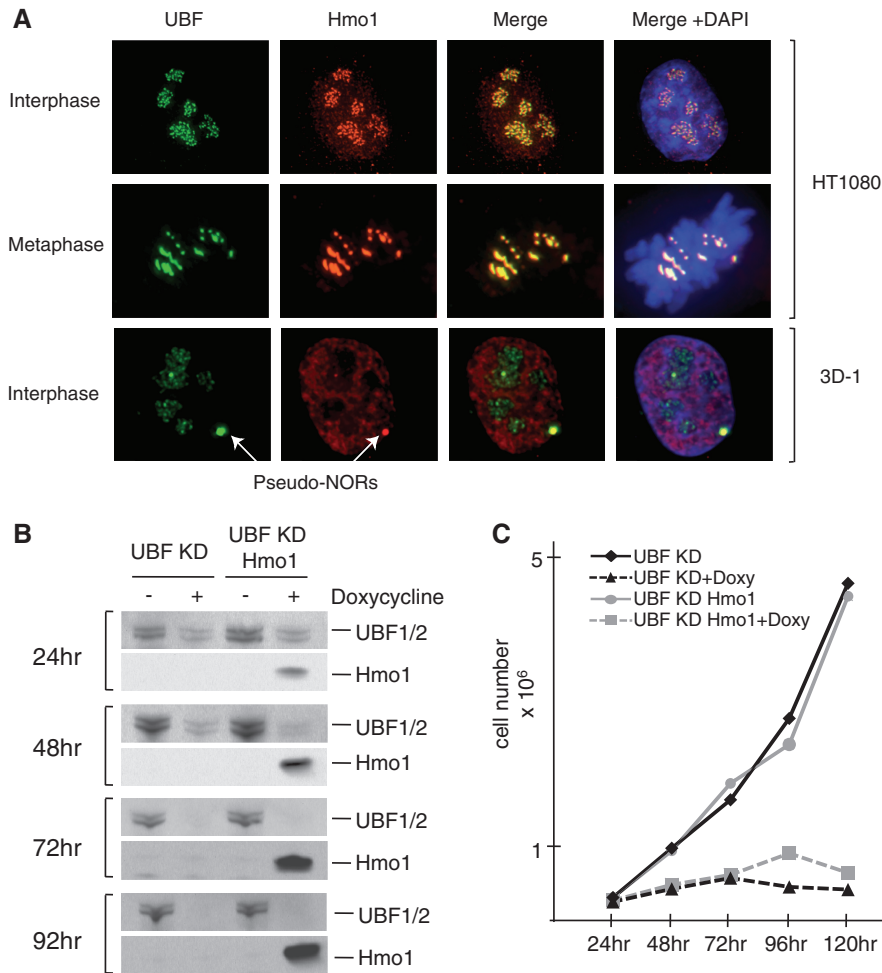
Figure 7. Hmo1 is unable to fulfill UBF1 essential function(s) in human cells. (**A**) Hmo1 expressed in the human cell line HT1080 is mostly colocalized with UBF in nucleoli (upper panel). Hmo1 produced in the human cell line 3D-1 is concentrated in Pseudo-NORs with UBF1 (lower panel). (**B**) shRNA targeting both UBF1 and UBF2 in the human cell line HT1080 was used to mediate their depletion. Western blotting was used to assess depletion efficiency and Hmo1 expression after doxycycline induction. (**C**) Growth curves after induction of Hmo1 expression and depletion of UBF (UBF KD Hmo1+doxy) and after only UBF depletion (UBF KD+ doxy) or without doxycycline (UBF KD Hmo1) (UBFKD) show that Hmo1 cannot overcome the growth arrest associated with UBF depletion.

mammal specific functions that cannot be complemented by Hmo1 expression.

In conclusion, both UBF1 and Hmo1 have the ability to colocalize with rDNA and seem to share a conserved ancestral function in Pol I transcription. However, in mammals, Hmo1 is unable to fulfill UBF1 essential function(s).

Pol I stimulation by Hmo1 requires the integrity of BoxA and the conserved motif

The organization of Hmo1 into three domains has been previously described: BoxA (aa 12–90) is a poorly conserved HMG Box required for dimerization, BoxB (aa 106–189) is a conserved HMG Box and BoxC (aa 219–246) is a highly charged motif involved in DNA bending (46). Our alignment between Hmo1 and UBF1 suggested the existence of a fourth domain in Hmo1 between BoxB and the C-terminal charged domain, a CR (aa 189–219) (Figure 8A). We generated a set of

Hmo1 truncations to delineate the functional importance of these four domains. We generated C-terminal, internal and N-terminal deletion mutants of Hmo1 (Figure 8A): BoxA comprising only the first 90 residues of Hmo1, BoxAB including the most conserved HMGB, Hmo1ΔCR containing an internal deletion spanning the CR, Hmo1ΔBoxA lacking N-terminal tail and Hmo1ΔC mutation removing the last 36 residues, which has been previously shown to induce no growth phenotype (20). We verified the expression of all deletion constructs using antibody against Hmo1 (Supplementary Figure S2B). We defined their intracellular localization and their involvement in Pol I stimulation and RPG transcription expressing them in *hmo1Δ-rpa49Δ* or *hmo1Δ-rps23bΔ* strains (Figure 8).

Because Hmo1 could dimerize *in vitro* (46), we first tested localization of YFP N-terminally tagged constructs, in absence of endogenous Hmo1 (Figure 8B). All constructs lacking charged C terminal motif were both nuclear and cytoplasmic with no nucleolar accumulation.
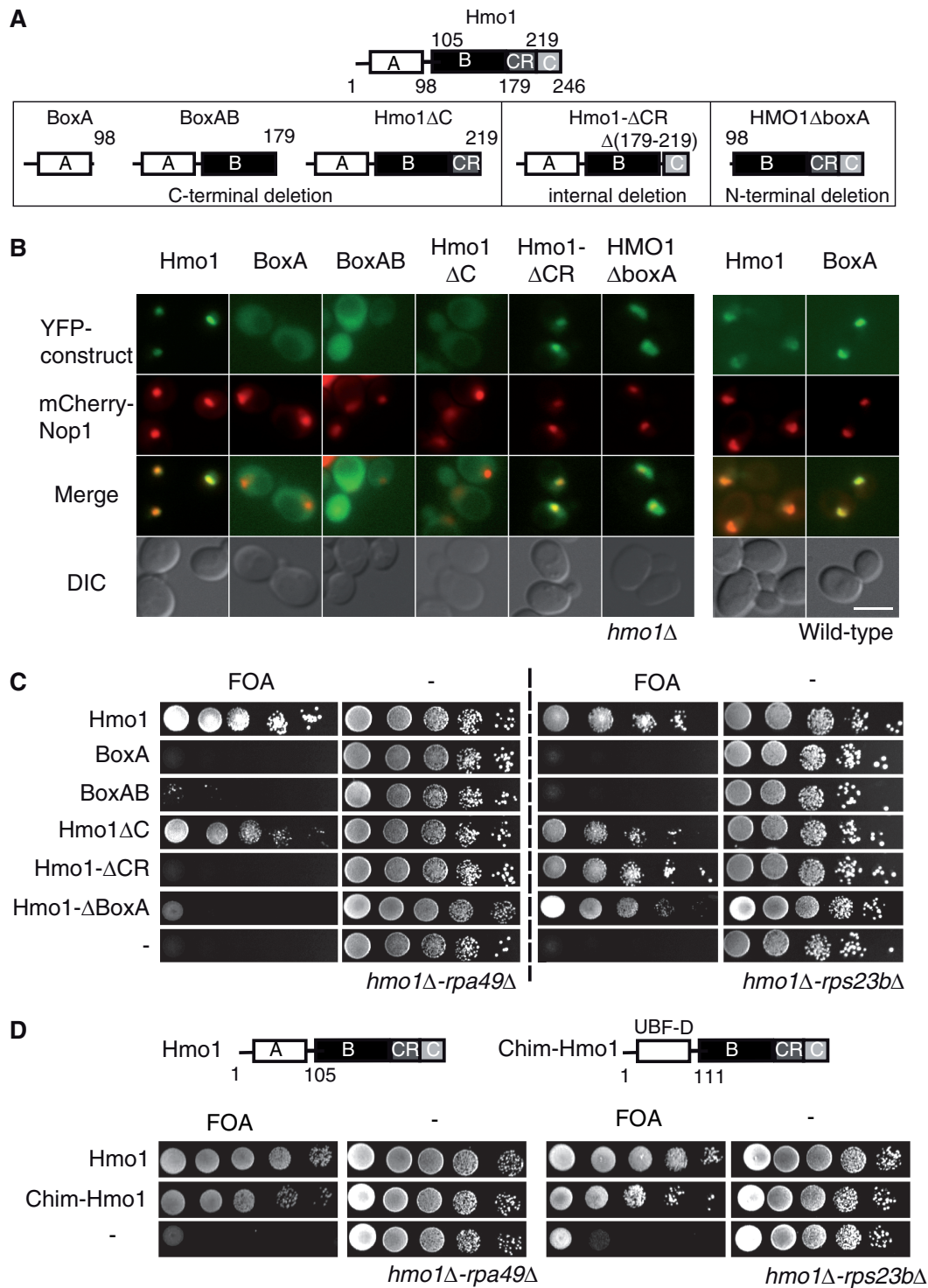
Figure 8. Pol I stimulation by Hmo1 requires the integrity of BoxA and the conserved motif CR. (**A**) Schematic representation of five truncated versions of Hmo1: BoxA, BoxAB, Hmo1ΔCR and Hmo1ΔBoxA. Hmo1 full size is represented on the top. Location of domains [BoxA (A), BoxB (**B**), CR, C terminal tail (**C**)] is indicated for each construct. (**B**) The five truncated versions of Hmo1, BoxA, BoxAB, Hmo1ΔCR, Hmo1ΔC and Hmo1ΔBoxA were YFP fused and expressed in an *hmo1Δ* background bearing nucleolar (mCherry-Nop1) and nuclear pore complex (CFp-Nup49) markers. Full size Hmo1 and BoxA were expressed in a WT strain bearing nucleolar (mCherry-Nop1) and nuclear pore complex (CFP-Nup49) markers. Selected cells are representative of the population. Scale bar = 5μm (**C**) The truncated Hmo1 constructions presented in the upper panel were functionally tested. Ten-fold serial dilutions of *hmo1Δ-rpa49Δ* (left) and *hmo1Δ-rps23bΔ* (right) strains expressing Hmo1 (Hmo1), or the four truncated constructions BoxA, BoxAB, Hmo1ΔC, Hmo1ΔCR or an empty vector (−) were spotted on plates containing 5-FOA to test for complementation. (**D**) The Hmo1 Box A can be functionally exchanged with the UBF1 dimerization motif. The BoxA of Hmo1 was swapped with the UBF1 dimerization motif to generate a chimeric protein Chim-Hmo1. Ten-fold serial dilutions of *hmo1Δ-rpa49Δ* (left) and *hmo1Δ-rps23*bΔ (right) strains expressing Hmo1 (Hmo1), Chim-Hmo1 or an empty vector (−) were spotted on plates containing 5-FOA to test for complementation.

Importantly, untagged Hmo1 lacking the C terminal domain is localized like the YFP-tagged construct (Supplementary Figure S3). Conversely, Hmo1ΔCR and Hmo1ΔBoxA were accumulated in the nucleus/nucleolus, strongly suggesting that C-terminus is necessary for nuclear/nucleolar localization. To directly test dimerization with endogenous Hmo1, we next expressed the different truncated versions of Hmo1 in presence of endogeneous Hmo1, i.e. in a WT strain also expressing mCherry-Nop1 (Hmo1-BoxA depicted in Figure 8B, data not shown). When comparing localizations with or without endogeneous Hmo1, Hmo1ΔBoxA localization was unaffected, whereas the three deletions bearing BoxA but lacking the C terminal domain were not anymore cytoplasmic but concentrated in the nucleus/ nucleolus in presence of Hmo1 (Figure 8B), suggesting a nucleolar localization driven by a piggyback mechanism (i.e. the YFP-BoxA protein heterodimerizes with endogenous Hmo1). BoxA acts like a dimerization motif.

We next expressed the five untagged deletion constructs in two mutants in which Hmo1 is essential, *hmo1Δ-rpa49Δ* and *hmo1Δ-rps23bΔ*. Hmo1 full length and Hmo1ΔC suppressed lethality in both backgrounds, whereas BoxA and BoxAB constructs did not complement the double mutations. Interestingly, Hmo1ΔBoxA and Hmo1ΔCR could not complement the absence of Hmo1 in the *rpa49Δ* strain but could restore growth in the *hmo1Δ-rps23bΔ* mutant (Figure 8C). Pol I stimulation by Hmo1 requires the integrity of BoxA and the conserved motif.

A dimerization module in the N-terminus of UBF1 was previously identified (47), and our localization data suggest that Hmo1 N-terminus could also behave as a dimerization module *in vivo* (Figure 8B), supporting a previous biochemical study (46). Despite a lack of sequence similarity, BoxA and UBF1-N-terminus could have a similar function. To test this functional similarity, we swapped the BoxA of Hmo1 with the dimerization module of UBF1 (Figure 8D). Expression of Chim-hmo1 rescued the growth phenotype in both mutants: *hmo1Δ-rpa49Δ* and *hmo1Δ-rps23bΔ* (Figure 8D), whereas Hmo1 lacking BoxA did not restore the growth of the *hmo1Δ-rpa49Δ* strain. The N-terminal dimerization motif in Hmo1 seems to be necessary to stimulate Pol I transcription.

In conclusion, some of the functions of Hmo1 are fulfilled in absence of the conserved domain CR or of the dimerization motif as shown in *rps23bΔ* mutant. Conversely, Pol I stimulation by Hmo1 requires the integrity of the dimerization motif and the CR. Canonical HMGB BoxB of Hmo1 is essential in both tested mutants *hmo1Δ-rpa49Δ* and *hmo1Δ-rps23bΔ*.

DISCUSSION

In this manuscript, we report *in vivo* structure-function analysis of the *S. cerevisiae*'s transcription factor Hmo1. HMGB Box proteins Hmo1 in yeast and UBF1 in human both stimulate Pol I, and it was suggested that they could be functionally related (14). In our study, we clarify this point. We have characterized a functional conservation between the human UBF1 and Hmo1 in stimulating rDNA transcription, and we have identified Sp-Hmo1, an ortholog in another eukaryotic organism, *S. pombe*. Hmo1, UBF1 and Sp-Hmo1 appear to have some interchangeable activities in stimulating Pol I transcription. However, although Hmo1 has multiple functions *in vivo*, including regulation of RPG expression, UBF1 and Sp-Hmo1 are unable to stimulate RPG expression, as judged by their failure to rescue of *hmo1Δ rps23bΔ* lethality (Figures 2D and 5E). Such partial complementation suggested that Hmo1's activities could be uncoupled.

Hmo1 and UBF1 are not equivalent but share a common function in rDNA transcription

Hmo1 has been implicated in genome stability, transcription by RNA pol II (20,22–25), and we have shown here that Hmo1 shares a common function with UBF1 during RNA pol I transcription. In metazoans, UBF is a multifunctional protein involved in both initiation and elongation of rDNA transcription (8,11). We propose that HMGB proteins do not stimulate preferentially initiation rate, but also act during elongation, most likely stimulating processivity of the Pol I enzyme. Two lines of evidence support this hypothesis. First, UBF1 interaction with the initiation factor SL1 requires its C-terminal region (42), whereas when expressed in yeast, the UBF1 N-terminal domain is sufficient to complement Hmo1 function in a Pol I mutant. Therefore, the conserved function between HMGB is unlikely to be the interaction with initiation factors. Second, it is well established that human UBF and budding yeast Hmo1 are localized along the entire Pol I transcribed region of the rRNA genes (3,4,24). On UBF1 expression or Hmo1 overexpression, rRNA synthesis is stimulated without any evidence of preferential stimulation of initiation, i.e. Pol I loading rate per gene and its density on the 5' end of the transcription unit relative to 3' are not significantly modified.

What could be the function of the domains of these HMGB proteins?

Alignments between Hmo1, UBF N-terminal domain and Sp-Hmo1 are shown in Figure 9. Hmo1 could be divided in four domains: the N-terminal region BoxA required for dimerization, BoxB including a consensus HMG Box, a CR of 40 amino acids and a C-terminal region rich in lysine residues. Interestingly, Hmo1's BoxA, BoxB and CR domains that have counterparts either in human and/or in *S. pombe* are all required for stimulating Pol I *in vivo*. Hmo1's deletion mutants lacking either BoxA or CR domain can still stimulate transcription of a tested RPG gene.

Hmo1's BoxA was initially described as a degenerated HMGB Box (48). Hmo1 BoxA and UBF dimerization module have similar size. We show here that Box A could be swapped with UBF's dimerization domain, which does not have HMGB properties. This suggests that BoxA is primarily a dimerization module, with no essential DNA binding function. Alignment also reveals a conservation of basic properties of the linker region
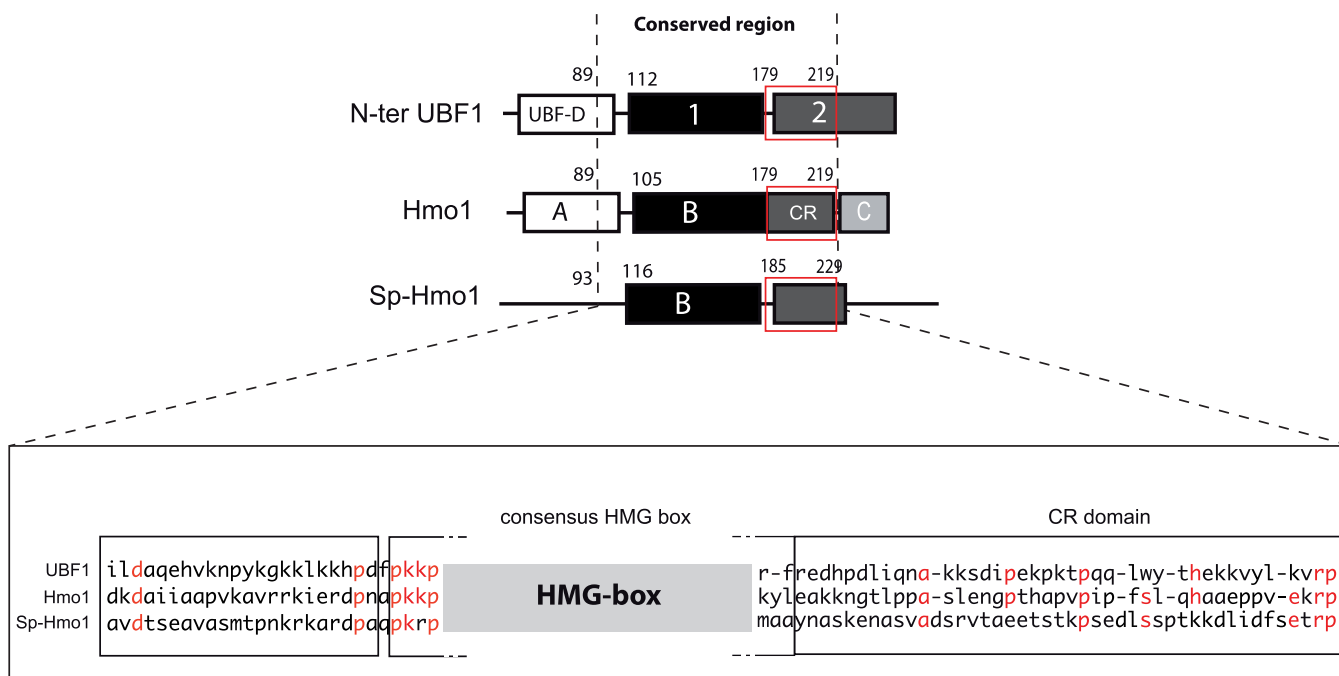
Figure 9. Domain organization of Hmo1. Schematic representation of N-terminal part of UBF1, Hmo1 and Sp-Hmo1 containing a dimerization motif, a consensus HMG Box motif and a CR similar to the beginning of Box2 of UBF1. A part of the amino acid composition of these three domains is shown in the close-up view (dotted line; lower panel). Position of consensus HMGB is indicated, followed by the CR domain. Residues that are identical are in red.

between BoxA and HMGB motif (Figure 9). The canonical HMGB BoxB is essential for all tested Hmo1 functions. Basic residues located just before HMGB BoxB are known to stabilize bending triggered by adjacent HMGB motif (49) and are essential for DNA-bending activity of UBF1 (13). Self-association of HMGB proteins is particularly important to form loop structures: Hmo1-ΔBoxA fails to bend DNA and UBF1 without dimerization module loses the ability to form a loop structure called enhancesome (13,48).

The other essential domain identified in this study to stimulate rDNA transcription is a CR. Interestingly, UBF phosphorylation in this region (residue 201) alters significantly its ability to form enhancesome structure (50). By analogy with UBF1, this motif in Hmo1 could also be involved in DNA looping.

C-terminal region rich in lysine residues of Hmo1 is not conserved and seems to act as a nucleolar targeting sequence. Known functions of Hmo1 require nuclear/nucleolar localization. Surprisingly, Hmo1ΔC lacking this domain is functional, in agreement with previous observations (20). Hmo1ΔC is predominantly cytoplasmic, but is not excluded from the nuclear/nucleolar sub compartments. We propose that the small size of Hmo1ΔC (25kDa) allows passive import in the nuclear/nucleolar compartment. We speculate that this minor pool is sufficient to fulfill Hmo1's functions.

CONCLUSIONS

In conclusion, Hmo1 has acquired species-specific functions and shares with UBF1 and Sp-Hmo1 an ancestral function to stimulate rDNA transcription. The

dimerization domain and CR from Hmo1 are required for DNA bending and confer the ability to form loop structure and potentially act on topological state of rDNA. We propose that Hmo1, Sp-Hmo1 and UBF1 regulate transcription elongation by modifying chromatin of active genes. Such activity might not be required for RPG regulation, as suggested by our genetic assay.

Active rDNA genes is at the same time a repeated region largely devoided of nucleosomal structure (3,4) and the most transcribed region of the eukaryotic genome. The conserved function of Hmo1 and UBF1 could be a topological function involved in regulation of chromatin structure of active rDNA. Further investigations will be necessary to fully understand stimulatory function of HMGB proteins.

SUPPLEMENTARY DATA

Supplementary Data are available at NAR Online, including [51–55].

REFERENCES

1. Lempiainen,H. and Shore,D. (2009) Growth control and ribosome biogenesis. *Curr. Opin. Cell. Biol.*, **21**, 855–863.
2. Albert,B., Perez-Fernandez,J., Leger-Silvestre,I. and Gadal,O. (2012) Regulation of ribosomal RNA production by RNA polymerase I: does elongation come first? *Genet. Res. Int.*, **2012**, 276948.
3. Merz,K., Hondele,M., Goetze,H., Gmelch,K., Stoeckl,U. and Griesenbeck,J. (2008) Actively transcribed rRNA genes in S. cerevisiae are organized in a specialized chromatin associated with the high-mobility group protein Hmo1 and are largely devoid of histone molecules. *Genes Dev.*, **22**, 1190–1204.
4. O'Sullivan,A.C., Sullivan,G.J. and McStay,B. (2002) UBF binding *in vivo* is not restricted to regulatory sequences within the vertebrate ribosomal DNA repeat. *Mol. Cell. Biol.*, **22**, 657–668.
5. O'Mahony,D.J. and Rothblum,L.I. (1991) Identification of two forms of the RNA polymerase I transcription factor UBF. *Proc. Natl. Acad. Sci. USA*, **88**, 3180–3184.
6. Kuhn,A., Voit,R., Stefanovsky,V., Evers,R., Bianchi,M. and Grummt,I. (1994) Functional differences between the two splice variants of the nucleolar transcription factor UBF: the second HMG box determines specificity of DNA binding and transcriptional activity. *EMBO J.*, **13**, 416–424.
7. Friedrich,J.K., Panov,K.I., Cabart,P., Russell,J. and Zomerdijk,J.C. (2005) TBP-TAF complex SL1 directs RNA polymerase I pre-initiation complex formation and stabilizes upstream binding factor at the rDNA promoter. *J. Biol. Chem.*, **280**, 29551–29558.
8. McStay,B., Hu,C.H., Pikaard,C.S. and Reeder,R.H. (1991) xUBF and Rib 1 are both required for formation of a stable polymerase I promoter complex in X. laevis. *EMBO J.*, **10**, 2297–2303.
9. Panov,K.I., Friedrich,J.K., Russell,J. and Zomerdijk,J.C. (2006) UBF activates RNA polymerase I transcription by stimulating promoter escape. *EMBO J.*, **25**, 3310–3322.
10. Sanij,E. and Hannan,R.D. (2009) The role of UBF in regulating the structure and dynamics of transcriptionally active rDNA chromatin. *Epigenetics*, **4**, 374–382.
11. Stefanovsky,V., Langlois,F., Gagnon-Kugler,T., Rothblum,L.I. and Moss,T. (2006) Growth factor signaling regulates elongation of RNA polymerase I transcription in mammals via UBF phosphorylation and r-chromatin remodeling. *Mol. Cell*, **21**, 629–639.
12. Mais,C., Wright,J.E., Prieto,J.L., Raggett,S.L. and McStay,B. (2005) UBF-binding site arrays form pseudo-NORs and sequester the RNA polymerase I transcription machinery. *Genes Dev.*, **19**, 50–64.
13. Stefanovsky,V.Y., Pelletier,G., Bazett-Jones,D.P., Crane-Robinson,C. and Moss,T. (2001) DNA looping in the RNA polymerase I enhancesome is the result of non-cooperative in-phase bending by two UBF molecules. *Nucleic Acids Res.*, **29**, 3241–3247.
14. Gadal,O., Labarre,S., Boschiero,C. and Thuriaux,P. (2002) Hmo1, an HMG-box protein, belongs to the yeast ribosomal DNA transcription system. *EMBO J.*, **21**, 5498–5507.
15. Hanada,K., Song,C.Z., Yamamoto,K., Yano,K., Maeda,Y., Yamaguchi,K. and Muramatsu,M. (1996) RNA polymerase I associated factor 53 binds to the nucleolar transcription factor UBF and functions in specific rDNA transcription. *EMBO J.*, **15**, 2217–2226.
16. Albert,B., Leger-Silvestre,I., Normand,C., Ostermaier,M.K., Perez-Fernandez,J., Panov,K.I., Zomerdijk,J.C., Schultz,P. and Gadal,O. (2011) RNA polymerase I-specific subunits promote polymerase clustering to enhance the rRNA gene transcription cycle. *J. Cell. Biol.*, **192**, 277–293.
17. Geiger,S.R., Lorenzen,K., Schreieck,A., Hanecker,P., Kostrewa,D., Heck,A.J. and Cramer,P. (2010) RNA polymerase I contains a TFIIF-related DNA-binding subcomplex. *Mol. Cell*, **39**, 583–594.
18. Beckouet,F., Labarre-Mariotte,S., Albert,B., Imazawa,Y., Werner,M., Gadal,O., Nogi,Y. and Thuriaux,P. (2008) Two RNA polymerase I subunits control the binding and release of Rrn3 during transcription. *Mol. Cell. Biol.*, **28**, 1596–1605.
19. French,S.L., Sikes,M.L., Hontz,R.D., Osheim,Y.N., Lambert,T.E., El Hage,A., Smith,M.M., Tollervey,D., Smith,J.S. and Beyer,A.L. (2010) Distinguishing the roles of Topoisomerases I and II in relief of transcription-induced torsional stress in yeast rRNA genes. *Mol. Cell. Biol.*, **31**, 482–494.
20. Lu,J., Kobayashi,R. and Brill,S.J. (1996) Characterization of a high mobility group 1/2 homolog in yeast. *J. Biol. Chem.*, **271**, 33678–33685.
21. Kasahara,K., Ki,S., Aoyama,K., Takahashi,H. and Kokubo,T. (2008) *Saccharomyces cerevisiae* HMO1 interacts with TFIID and participates in start site selection by RNA polymerase II. *Nucleic Acids Res.*, **36**, 1343–1357.
22. Kasahara,K., Ohtsuki,K., Ki,S., Aoyama,K., Takahashi,H., Kobayashi,T., Shirahige,K. and Kokubo,T. (2007) Assembly of regulatory factors on rRNA and ribosomal protein genes in *Saccharomyces cerevisiae*. *Mol. Cell. Biol.*, **27**, 6686–6705.
23. Hall,D.B., Wade,J.T. and Struhl,K. (2006) An HMG protein, Hmo1, associates with Promoters of many ribosomal protein genes and thoughout rRNA gene locus in *Saccharomyces cerevisiae*. *Mol. Cell. Biol.*, **26**, 3672–3679.
24. Berger,A.B., Decourty,L., Badis,G., Nehrbass,U., Jacquier,A. and Gadal,O. (2007) Hmo1 is required for TOR-dependent regulation of ribosomal protein gene transcription. *Mol. Cell. Biol.*, **27**, 8015–8026.
25. Bermejo,R., Capra,T., Gonzalez-Huici,V., Fachinetti,D., Cocito,A., Natoli,G., Katou,Y., Mori,H., Kurokawa,K., Shirahige,K. et al. (2009) Genome-organizing factors Top2 and Hmo1 prevent chromosome fragility at sites of S phase transcription. *Cell*, **138**, 870–884.
26. Sherman,F., Fink,G.R. and Hicks,J.B.N. (1986) *Methods in Yeast Genetics. A Laboratory Course Manual.* Cold Spring Harbor Laboratory, New York.
27. Forsburg,S.L. and Rhind,N. (2006) Basic methods for fission yeast. *Yeast*, **23**, 173–183.
28. Boeke,J.D., Lacroute,F. and Fink,G.R. (1984) A positive selection for mutants lacking orotidine-5'-phosphate decarboxylase activity in yeast:5-fluoro-orotic acid resistance. *Mol. Gen. Genet.*, **197**, 345–346.
29. Hermann-Le Denmat,S., Werner,M., Sentenac,A. and Thuriaux,P. (1994) Suppression of yeast RNA polymerase III mutations by FHL1, a gene coding for a fork head protein involved in rRNA processing. *Mol. Cell. Biol.*, **14**, 2905–2913.
30. Beltrame,M. and Tollervey,D. (1992) Identification and functional analysis of two U3 binding sites on yeast pre-ribosomal RNA. *EMBO J.*, **11**, 1531–1542.
31. Gulli,M.P., Girard,J.P., Zabetakis,D., Lapeyre,B., Melese,T. and Caizergues-Ferrer,M. (1995) gar2 is a nucleolar protein from Schizosaccharomyces pombe required for 18S rRNA and 40S ribosomal subunit accumulation. *Nucleic Acids Res.*, **23**, 1912–1918.
32. Berger,A.B., Cabal,G.G., Fabre,E., Duong,T., Buc,H., Nehrbass,U., Olivo-Marin,J.C., Gadal,O. and Zimmer,C. (2008) High-resolution statistical mapping reveals gene territories in live yeast. *Nat. Methods*, **5**, 1031–1037.
33. Rougemaille,M., Dieppois,G., Kisseleva-Romanova,E., Gudipati,R.K., Lemoine,S., Blugeon,C., Boulay,J., Jensen,T.H.,

Stutz,F., Devaux,F. *et al.* (2008) THO/Sub2p functions to coordinate 3′-end processing with gene-nuclear pore association. *Cell*, **135**, 308–321.

34. Hannan,R., Stefanovsky,V., Arino,T., Rothblum,L. and Moss,T. (1999) Cellular regulation of ribosomal DNA transcription:both rat and Xenopus UBF1 stimulate rDNA transcription in 3T3 fibroblasts. *Nucleic Acids Res.*, **27**, 1205–1213.

35. Smith,S.D., O'Mahony,D.J., Kinsella,B.T. and Rothblum,L.I. (1993) Transcription from the rat 45S ribosomal DNA promoter does not require the factor UBF. *Gene Expr.*, **3**, 229–236.

36. Gadal,O., Mariotte-Labarre,S., Chédin,S., Quemeneur,E., Carles,C., Sentenac,A. and Thuriaux,P. (1997) A34.5, a nonessential component of yeast RNA polymerase I, cooperates with subunit A14 and DNA topoisomerase I to produce a functional rRNA synthesis machine. *Mol. Cell. Biol.*, **17**, 1787–1795.

37. Panov,K.I., Panova,T.B., Gadal,O., Nishiyama,K., Saito,T., Russell,J. and Zomerdijk,J.C. (2006) RNA polymerase I-specific subunit CAST/hPAF49 has a role in the activation of transcription by upstream binding factor. *Mol. Cell. Biol.*, **26**, 5436–5448.

38. Russell,J. and Zomerdijk,J.C. (2006) The RNA polymerase I transcription machinery. *Biochem. Soc. Symp.*, **73**, 203–216.

39. Cioci,F., Vu,L., Eliason,K., Oakes,M., Siddiqi,I.N. and Nomura,M. (2003) Silencing in yeast rDNA chromatin: reciprocal relationship in gene expression between RNA polymerase I and II. *Mol. Cell*, **12**, 135–145.

40. Schneider,D.A., French,S.L., Osheim,Y.N., Bailey,A.O., Vu,L., Dodd,J., Yates,J.R., Beyer,A.L. and Nomura,M. (2006) RNA polymerase II elongation factors Spt4p and Spt5p play roles in transcription elongation by RNA polymerase I and rRNA processing. *Proc. Natl Acad. Sci. USA*, **103**, 12707–12712.

41. Schnapp,G., Santori,F., Carles,C., Riva,M. and Grummt,I. (1994) The HMG box-containing nucleolar transcription factor UBF interacts with a specific subunit of RNA polymerase I. *EMBO J.*, **13**, 190–199.

42. Jantzen,H.M., Chow,A.M., King,D.S. and Tjian,R. (1992) Multiple domains of the RNA polymerase I activator hUBF interact with the TATA-binding protein complex hSL1 to mediate transcription. *Genes Dev.*, **6**, 1950–1963.

43. Nakagawa,K., Hisatake,K., Imazawa,Y., Ishiguro,A., Matsumoto,M., Pape,L., Ishihama,A. and Nogi,Y. (2003) The fission yeast RPA51 is a functional homolog of the budding yeast A49 subunit of RNA polymerase I and required for maximizing transcription of ribosomal DNA. *Genes Genet. Syst.*, **78**, 199–209.

44. Roussel,P., Andre,C., Masson,C., Geraud,G. and Hernandez-Verdun,D. (1993) Localization of the RNA polymerase I transcription factor hUBF during the cell cycle. *J. Cell. Sci.*, **104 (Pt 2)**, 327–337.

45. Wittner,M., Hamperl,S., Stockl,U., Seufert,W., Tschochner,H., Milkereit,P. and Griesenbeck,J. (2011) Establishment and maintenance of alternative chromatin States at a multicopy gene locus. *Cell*, **145**, 543–554.

46. Xiao,L., Williams,A.M. and Grove,A. (2010) The C-terminal domain of yeast high mobility group protein HMO1 mediates lateral protein accretion and in-phase DNA bending. *Biochemistry*, **49**, 4051–4059.

47. McStay,B., Frazier,M.W. and Reeder,R.H. (1991) xUBF contains a novel dimerization domain essential for RNA polymerase I transcription. *Genes Dev.*, **5**, 1957–1968.

48. Kamau,E., Bauerle,K.T. and Grove,A. (2004) The *Saccharomyces cerevisiae* high mobility group box protein HMO1 contains two functional DNA binding domains. *J. Biol. Chem.*, **279**, 55234–55240.

49. Allain,F.H., Yen,Y.M., Masse,J.E., Schultze,P., Dieckmann,T., Johnson,R.C. and Feigon,J. (1999) Solution structure of the HMG protein NHP6A and its interaction with DNA reveals the structural determinants for non-sequence-specific binding. *EMBO J.*, **18**, 2563–2579.

50. Stefanovsky,V.Y., Pelletier,G., Hannan,R., Gagnon-Kugler,T., Rothblum,L.I. and Moss,T. (2001) An immediate response of ribosomal transcription to growth factor stimulation in mammals is mediated by ERK phosphorylation of UBF. *Mol. Cell*, **8**, 1063–1073.

51. Léger-Silvestre,I., Trumtel,S., Noaillac-Depeyre,J. and Gas,N. (1999) Functional compartmentalization of the nucleus in the budding yeast *Saccharomyces cerevisiae*. *Chromosoma*, **108**, 103–113.

52. Thiry,M. and Lafontaine,D.L. (2005) Birth of a nucleolus: the evolution of nucleolar compartments. *Trends Cell. Biol.*, **15**, 194–199.

53. Gadal,O., Strauss,D., Petfalski,E., Gleizes,P.E., Gas,N., Tollervey,D. and Hurt,E. (2002) Rlp7p is associated with 60S preribosomes, restricted to the granular component of the nucleolus, and required for pre-rRNA processing. *J. Cell. Biol.*, **157**, 941–951.

54. Baudin,A., Ozier-Kalogeropoulos,O., Denouel,A., Lacroute,F. and Cullin,C. (1993) A simple and efficient method for direct gene deletion in *Saccharomyces cerevisiae*. *Nucleic Acids Res.*, **21**, 3329–3330.

55. Pelloquin,L., Belenguer,P., Menon,Y., Gas,N. and Ducommun,B. (1999) Fission yeast Msp1 is a mitochondrial dynamin-related protein. *J. Cell Sci.*, **112 (Pt 22)**, 4151–4161.